RESEARCH ARTICLE

Semi-automated segmentation of magnetic resonance images for thigh skeletal muscle and fat using threshold technique after spinal cord injury

Mina P. Ghatas[1], Robert M. Lester[1], M. Rehan Khan[2], Ashraf S. Gorgey[1, 3, *]

1 Department of Spinal Cord Injury and Disorders, Hunter Holmes McGuire VA Medical Center, Richmond, VA, USA
2 Department of Radiology, Hunter Holmes McGuire VA Medical Center, Richmond, VA, USA
3 Department of Physical Medicine and Rehabilitation, Virginia Commonwealth University, Richmond, VA, USA

Funding: *This study was supported by the Department of Veteran Affairs, Veteran Health Administration, Rehabilitation Research and Development Service (B7867-W) and DoD-CDRMP (W81XWH-14-SCIRP-CTA) (to ASG).*

Abstract

Magnetic resonance imaging is considered the "gold standard" technique for quantifying thigh muscle and fat cross-sectional area. We have developed a semi-automated technique to segment seven thigh compartments in persons with spinal cord injury. Thigh magnetic resonance images from 18 men (18–50 years old) with traumatic motor-complete spinal cord injury were analyzed in a blinded fashion using the threshold technique. The cross-sectional area values acquired by thresholding were compared to the manual tracing technique. The percentage errors for thigh circumference were (threshold: 170.71 ± 38.67; manual: 169.45 ± 38.27 cm^2) 0.74%, subcutaneous adipose tissue (threshold: 65.99±30.79; manual: 62.68 ± 30.22) 5.2%, whole muscle (threshold: 98.18 ± 20.19; manual: 98.20 ± 20.08 cm2) 0.13%, femoral bone (threshold: 6.53 ± 1.09; manual: 6.53 ± 1.09 cm^2) 0.64%, bone marrow fat (threshold: 3.12 ± 1.12; manual: 3.1 ± 1.11 cm^2) 0.36%, knee extensor (threshold: 43.98 ± 7.66; manual: 44.61 ± 7.81 cm^2) 1.78% and % intramuscular fat (threshold: 10.45 ± 4.29; manual: 10.92 ± 8.35%) 0.47%. Collectively, these results suggest that the threshold technique provided a robust accuracy in measuring the seven main thigh compartments, while greatly reducing the analysis time.

Key Words: *spinal cord injury; magnetic resonance imaging; semi-automated segmentation; subcutaneous adipose tissue; intramuscular fat*

Correspondence to:
Ashraf S. Gorgey, MPT, PhD, FACSM, ashraf.gorgey@va.gov.

orcid:
0000-0002-9157-6034 (Ashraf S. Gorgey)

doi: *10.4103/1673-5374.238623*

Accepted: *2018-07-12*

Introduction

After spinal cord injury (SCI), sedentarism and decreased level of physical activity result in extensive skeletal muscle atrophy and increased adiposity below the level of injury (Elder et al., 2004; Gorgey and Dudley, 2007). Magnetic resonance imaging (MRI) has emerged as the "gold-standard" technique for quantifying thigh skeletal muscle and fat compartments (Mitsiopoulos et al., 1985; Gorgey et al., 2013b, 2017a) and is ideally suited for measuring body composition outcomes of clinical trials investigating the effects of exercise intervention after SCI (Gorgey et al., 2012, 2013a). Additionally, MRI allows for accurate measurement of cortical bone and bone marrow fat which is important for SCI patients whom exhibit increased prevalence of osteoporosis and risk of fractures of lower extremity bone (Wilmet et al., 1996; Elder et al., 2004; Eser et al., 2004; Gorgey and Dudley, 2007; Qin et al., 2010; Fattal et al., 2011; Dudley-Javoroski and Shields, 2012). In vivo measurement of skeletal muscle, fat and bone compartments is of paramount importance to this population because of decreased fat-free mass after SCI. This is likely to influence basal metabolic rate (BMR) which may be as low as 1200 kcal/d, resulting in a detrimental energy imbalance and increased prevalence of obesity with increased regional and whole-body adiposity (Buchholz et al., 2003; Gater, 2007; Lester et al., 2017). Reduction in muscle size is also associated with metabolic abnormalities similar to chronic obesity, insulin resistance, dyslipidemia, type II diabetes mellitus and cardiovascular disease (Duckworth et al., 1980; Phillips et al., 1998; Elder et al., 2004; Gater, 2007; Gorgey and Dudley, 2007; Gorgey et al., 2015). Moreover, skeletal muscle atrophy is accompanied with infiltration of intramuscular fat (IMF) that may explain 70% of the variance in impaired glucose tolerance in persons with SCI (Elder et al., 2004). Therefore, accurate quantification of the magnitude of skeletal muscle atrophy and fat infiltration may help to explain the decreased levels of BMR and secondary health consequences after SCI.

Manual segmentation, in which muscle groups are traced directly along anatomical borders, is considered one of the most reliable means of segmentation (Gorgey and Dudley, 2007; Lester et al., 2017). However, manual tracing may be influenced by the visual subjectivity of the analyst. This subjectivity may introduce sources of error considering the volume of data when analyzing multi-axial slices at multiple time points. Moreover, subjectivity may stem from poor image quality or extensive IMF infiltration, making the delineation of anatomical borders more difficult (Modlesky et al., 2004). In addition, manual tracing requires considerable time to analyze multi-axial images in larger clinical trials (Lester et al., 2017). Equivocal evidence suggests that manual tracing of thigh muscle and fat compartments may require ~1–1.5 years to complete in a sample size of 20 persons with SCI (Gorgey et al., 2011a). This may lead to reliance on alternative methods of quantifying body composition, similar to dual-energy

X-ray absorptiometry, which may under-predict fat-free mass in persons with SCI (Modlesky et al., 2004). Additionally, dual-energy X-ray absorptiometry is limited in its ability to distinguish between subcutaneous adipose tissue (SAT) and ectopic adipose tissue, a major distinction when evaluating metabolic health after SCI (Gorgey et al., 2015).

The threshold technique was designed to reduce the influence of human subjectivity as well as reduce the time needed for analysis, while maintaining a robust accuracy of measuring body compartments (Schick, 2016). A previous study used automated threshold segmentation to quantify percentage-subcutaneous adipose tissue (%SAT) of the lower extremities to determine associations between %SAT and monogenic metabolic syndrome subtypes in abled-bodied subjects. The study reported significant differences in the amounts of SAT between the two monogenic subtypes, with less SAT in the subtype 2 subject, compared to subtype 3 (Al-Attar et al., 2006). Additionally, threshold techniques were used to quantify IMF which may be a biomarker of osteoarthritis incidence and progression (Prescott et al., 2009). In combination with morphological constraints specificity of IMF segmentation was improved while maintaining the sensitivity of the automated technique (Prescott et al., 2009). Others have used a threshold algorithm to assess paraspinal muscle composition as reports suggest an association between muscle degeneration and lower back pain in abled-bodied individuals (Fortin et al., 2017). Automated threshold techniques may be difficult to use in evaluating thigh compartments in persons with SCI, considering the extensive muscle atrophy and infiltration of IMF.

The purpose of the current manuscript was to validate the use of a semi-automated threshold technique against the standard manual tracing technique previously used to measure thigh muscle compartments after SCI. Our objective was to present an accurate and robust tool of segmenting different thigh compartments after SCI.

Participants and Methods

Participants

Participants, including veterans and non-veterans from the greater Richmond, VA area, provided written informed consent before enrollment in the study. All study procedures were approved by the Institutional Review Board (McGuire IRB#1) and conducted according to the *Declaration of Helsinki*. MRI images of the right thigh from 20 men (age, 36 ± 10 years; weight, 77.7 ± 12.0 kg; height, 1.78 ± 0.05 m; body mass index (BMI), 24 ± 4 kg/m^2; time since injury, 8 ± 7 years) with traumatic motor-complete SCI (C5-T11, American Spinal Injury Association (AIS) A or B) were captured as a part of a parent clinical trial registered at ClinicalTrials.gov (NCT01652040) (Gorgey et al., 2017a). To achieve our purpose a crossover design was implemented, such that images captured from the parent study were processed using two distinct methods described below. Two participants were excluded from this study because of heterotrophic ossification and movement artifact as result of involuntary muscle spasms that impacted image quality.

T1-weighted MRI

T1-weighted MR images were obtained from a totally body General Electric Signa 1.5-T (Waukesha, WI, USA) MRI (FSE; TR 850-1000 ms; TE 6.7 ms, NEX 1, TE length 3, flip angle 90, field of view (FOV) 20 cm; matrix size 256 × 256). Participants were instructed to lay in a supine position with legs strapped to avoid movement from involuntary muscle spasms. Twelve trans-axial images, slice thickness 8 mm with 16 mm interspace gap, were captured to cover the region from the hip to the knee joints of the right leg. Scan time was ~3.5 minutes to complete the entire scan. For simplicity, only the right thigh was considered for this study, because evidence suggests a negligible difference in muscle CSA between the right and left thighs in persons with motor-complete SCI (Castro et al., 1999) .

Manual tracing technique

Manual tracing segmentation was conducted using a commercially available software WinVessel (Version 2.011; written by Ronald Meyer at Michigan State University, Lansing, MI). Six ROIs which includes thigh circumference (TC), SAT, whole muscle (WM), femoral bone, bone marrow fat (BMF) and knee extensor (KE) CSAs were quantified by manually tracing along anatomical borders. Absolute IMF CSA was quantified using the midpoint between muscle and fat peaks of a bimodal histogram (Gorgey and Dudley, 2007; Lester et al., 2017). TC refers to the total CSA of the thigh just beneath the dermal layer including SAT, muscle, IMF and femoral bone. SAT is classified as the adipose tissue layer directly beneath the dermal layer of the skin and adjacent to the fascia lata and muscle wall of the thigh (Gorgey et al., 2011a, b). WM refers to the CSA of the total muscle mass of the thigh including IMF, located between SAT and the femoral bone. Bone refers to the total CSA of the femoral bone including outer cortical bone and bone marrow (Gorgey et al., 2013b). BMF refers to the CSA of adipose tissue within the femoral bone. KE refers to the total CSA of 4 heads including the vastus medialis, vastus intermedius, vastus lateralis and rectus femoris muscles. IMF refers to the fat infiltrated within the total muscle CSA and is presented as absolute and percentage. The sum of pixels within a bounded region was multiplied by the (FOV/matrix size)^2 to calculate the CSA of the ROI. **Figure 1** presents each ROI and the adjacent structures that were analyzed with manual and semi-automatic segmentation techniques.

Threshold segmentation of TC, WM, femoral bone, BMF and IMF

In ImageJ, prior to any segmentation procedures, all images underwent brightness/contrast enhancement using a contrast control tool to increase image quality and enhance background separation as much as possible. All image dynamics were converted to 8-bits to fit the requirements of ImageJ 1.50 (www.nih.gov) configuration. Moreover, a sharpening mask was applied to all images; the mask highlighted all pixels with relatively high signal intensity (*i.e.* SAT, IMF and BMF) and designated all other pixels with

lower signal intensity (*i.e.* muscle and bone) as background (**Figure 2A**). Thresholding was then applied, the values were automatically set (using the auto-threshold tool) to include only regions having pixels with high intensity levels, that isolated SAT, IMF and BMF from the remaining tissues. Above mentioned steps were applied only one time for each MRI sequence (each participant).

For each ROI, an edge detection tool was then used to differentiate between multiple objects having similar pixel intensity. The edge detection tool isolated all pixels having discontinuity in signal intensity to form one boundary (**Figure 2B, C**). The outer and inner SAT borders were determined using the edge detection tool. The outer border was then used to quantify the TC as shown in **Figure 2B**, whereas the inner border adjacent to the fascial line was used to quantify WM CSA.

The fascial line is the thick sheath of fibrous tissue enclosing the WM ROI of the thigh and serves as a critical anatomical reference separating SAT from muscle/intramuscular fat compartments; however, because fascia is characterized by low pixel intensity compared to SAT; it is difficult to accurately segment it using the threshold technique. To overcome this problem, the current method relies more on a geometrical structure determined by a convex hull algorithm. The convex hull of a set of points (*i.e.* thigh pixels) is the smallest convex polygon that contains all the points without any self-intersection; it can be visualized as the shape enclosed by a rubber band stretched around set of points (Barber et al., 1996). The convex hull algorithm was applied to the outer border of the muscle region to predict the fascial line, allowing for the differentiation of WM from SAT (**Figure 2D**).

To quantify WM CSA, first, an edge detection tool was used to trace the outer border of the muscle mass as shown in **Figure 2C**. Selection of the inner SAT border isolated muscle and IMF. Based on the assumption that the fascial line is adherent to the muscle mass of the thigh, the convex hull algorithm was used to mimic the borders of the fascial line and quantify WM CSA. To segment the femoral bone and bone marrow fat, the threshold values were set to include all pixel intensities higher than the dark region of the cortical bone (*i.e.* muscle, SAT, BMF and IMF). That enabled us to isolate the femoral bone from the adjacent thigh tissues. The edge detection tool was then used to generate a clear border surrounding the femoral bone and the bone marrow fat as shown in **Figure 2E**.

For IMF quantification, ten participants were randomly selected (age, 33.4 ± 10 years; weight, 75 ± 11 kg; height, 1.79 ± 0.06 m; BMI, 23 ± 3.5 kg/m^2; time since injury, 9 ± 8 years). Within the WM ROI (convex hull), threshold values were set to include all high intensity pixels that included both IMF and BMF. The BMF CSA was then subtracted to quantify absolute IMF CSA.

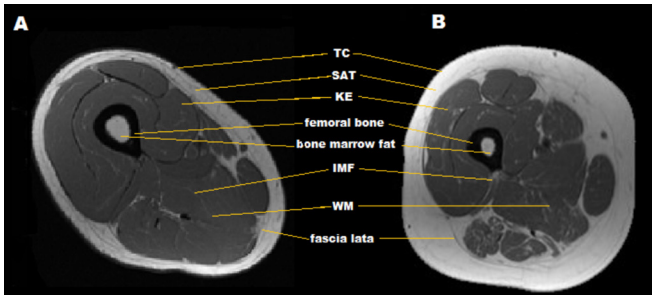

Figure 1 T1-weighted thigh magnetic resonance imaging (MRI).
(A) T1-weighted MRI of thigh in SCI individual with lower SAT and skeletal muscle atrophy. (B) T1-weighted MRI of thigh in person with SCI showing extensive skeletal muscle atrophy, SAT and IMF infiltration. TC: Thigh circumference; SAT: subcutaneous adipose tissue; WM: whole muscle; KE: knee extensor; IMF: intramuscular fat.

Semi-automated segmentation of the knee extensor (KE) muscle group

To measure the KE, 10 participants (age, 33 ± 10 years; weight, 77.0 ± 9 kg; height, 1.78 ± 0.05 m; BMI, 24 ± 3 kg/m^2; time since injury, 6 ± 5 years) were randomly selected to validate the semi-automatic segmentation technique against the manual tracing technique. Because individual muscle groups do not have distinct pixel intensity borders, nor a uniform geometrical structure to separate them from other muscle groups, segmentation was conducted using the segmentation editor plug-in for ImageJ, which uses a distance mapping algorithm to interpolate muscle borders. The borders of the KE muscle group were manually traced in three images located at the beginning, middle and end of the thigh sequence. The plug-in was then used to predict the KE borders of the remaining nine images in the sequence for a

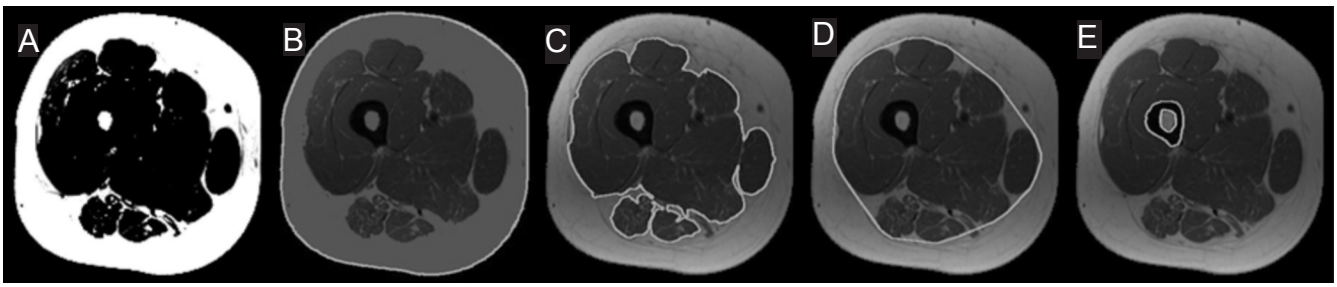

Figure 2 Magnetic resonance imaging (MRI) semi-automated segmentation.
(A) A high pass filter. (B) The outer SAT border used to quantify the TC CSA. (C) Segmentation of outer border of the muscle mass. (D) The convex hull applied to the outer border of the muscle mass to mimic fascial line. (E) Threshold segmentation of the femoral bone and bone marrow fat. TC: Thigh circumference; SAT: subcutaneous adipose tissue.

total of 12 images analyze. The anatomical borders of the KE muscle group, adjacent to both femoral bone and SAT were used as initial training regions to guide the interpolation algorithm to generate a higher accuracy of border prediction and segmentation.

Statistical analysis

All values were presented as mean ± SD. Computed CSAs derived from the threshold and border prediction techniques were compared to manual segmentation values. The CSAs for each ROI, across each of the 12 MRI slices, were averaged over the total number of participants for both manual and threshold techniques. Average (Av.) values were computed using the following equation, where n = number of participants:

$$\text{Av. CSA}_{(\text{ROI,image})} = \frac{\sum_1^n \text{CSA}_{(\text{ROI,image})}}{n}$$

Distributions of CSA along the MRI sequence from the hip to the knee joints, for both techniques are presented as scatter plots. Percentage error between manual (Mn) and threshold (Th) CSA values was calculated using the following equation:

$$\%\ \text{error} = \frac{|\text{CSA}_{(\text{Mn})} - \text{CSA}_{(\text{Th})}|}{\text{CSA}_{(\text{Mn})}} \times 100$$

Pearson's correlation coefficients were conducted to examine the relationships between manual tracing and semi-automated segmentation techniques. The average CSA of each participant in the manual vs. semi-automated segmentation techniques was used to ensure that the assumption of independency is not violated.

Results

CSA axial distribution

The average CSA distribution across the MRI sequence obtained from both techniques are presented in **Table 1** and **Figure 3**. Each ROI showed a similar trend and strong agreement throughout the sequence. The average percentage error for TC CSA was 0.74% (threshold: 170.71 ± 38.67 and manual: 169.45 ± 38.27 cm^2). the average percentage error for SAT CSA was 5.22% (threshold: 65.99 ± 30.79 and manual: 62.68 ± 30.22). The average percentage error for WM CSA was 0.14% (threshold: 98.19 ± 20.19 and manual: 98.09±20.08 cm^2). The average percentage error for femoral bone CSA (threshold: 6.51 ± 1.08 and manual: 6.53 ± 1.09 cm^2) was 0.34%. The average percentage error for KE CSA was 1.78% (threshold: 43.89 ± 7.67 and manual: 44.61 ± 7.81 cm^2). The average percentage error for BMF CSA was 0.64% (threshold: 3.12 ± 1.12 and manual: 3.1 ± 1.11 cm^2). The average percentage error for IMF CSA was 1.8% (threshold: 10.01 ± 2.65 and manual: 9.90 ± 5.25).

Bland-Altman plots

Figure 4 demonstrates a high level of agreement between the threshold and manual tracing techniques for TC (mean bias = –1.25 cm^2), SAT (mean bias = –3.30 cm^2; **Figure 4B**), WM (mean bias = –0.11 cm^2), BMF (mean bias = –0.33 cm^2), IMF (mean bias = –0.1 cm^2), and femoral bone (mean bias = 0.02 cm^2; **Figure 4D**), KE (mean bias = 0.71 cm^2; **Figure 4E**) and %IMF (mean bias = 0.4 cm^2) CSAs.

Table 1 Average mean (Av.), standard deviation (SD) and percentage error for TC, SAT, WM, femoral bone, KE, BMF cross-sectional area (cm^2) and %IMF for both Mn and Th techniques

ROI	Av.	Percentage error (%)
$TC_{(Th)}$	170.71 ± 38.67	0.74
$TC_{(Mn)}$	169.45 ± 38.27	
$SAT_{(Mn)}$	62.68 ± 30.22	5.22
$SAT_{(Mn)}$	65.99 ± 30.79	
$WM_{(Th)}$	98.18 ± 20.19	0.13
$WM_{(Mn)}$	98.20 ± 20.08	
$Bone_{(Th)}$	6.51 ± 1.08	0.36
$Bone_{(Mn)}$	6.53 ± 1.09	
$KE_{(Th)}$	43.98 ± 7.66	1.90
$KE_{(Mn)}$	44.61 ± 7.81	
$BMF_{(Th)}$	3.12 ± 1.12	0.64
$BMF_{(Mn)}$	3.10 ± 1.11	
$IMF_{(Th)}$	10.01 ± 2.65	1.80
$IMF_{(Mn)}$	9.90 ± 5.25	
$\%IMF_{(Th)}$	10.45 ± 4.29	0.47*
$\%IMF_{(Mn)}$	10.92 ± 8.35	

*Percentage difference for %IMF. TC: Thigh circumference; SAT: subcutaneous adipose tissue; WM: whole muscle; KE: knee extensor; BMF: bone marrow fat; %IMF: percentage intramuscular fat; Mn: manual; Th: threshold.

Linear regression

Figure 5 shows the relationships between the manual and threshold techniques for each ROI. Pearson's correlation coefficients of TC, SAT, WM, femoral bone, BMF, KE (n = 10 subjects), IMF (n = 10 subjects) and %IMF (n = 10 subjects) were r = 0.99 (P = 0.0001), r = 99 (P = 0.0001), r = 0.99 (P = 0.0001), r = 0.99 (P = 0.0001), r = 0.99 (P = 0.0001), r = 0.74 (P = 0.015) and r = 0.85 (P = 0.015), respectively.

For processing time, both investigators were asked to recall time needed to segment the seven ROIs; manual segmentation required ~25 minutes per image or ~5 hours per subject. In comparison, the technique required less than one hour to finish a whole sequence, demonstrating an 80% reduction in analysis time.

Discussion

The primary findings indicated that the threshold technique is accurate in quantifying TC, SAT, WM, femoral bone, BMF, KE and IMF CSAs and equivalent to the manual tracing technique in 18 men with SCI. The results showed a high level of agreement between the threshold and manual tracing techniques, highlighting that the threshold technique can robustly quantify muscle, fat and bone compartments in persons with SCI. SAT and %IMF has the wider levels of agreement compared to the other regions of interest. Despite the wider level of agreement in SAT and %IMF, the results were acceptable considering the difficulty in evaluating both

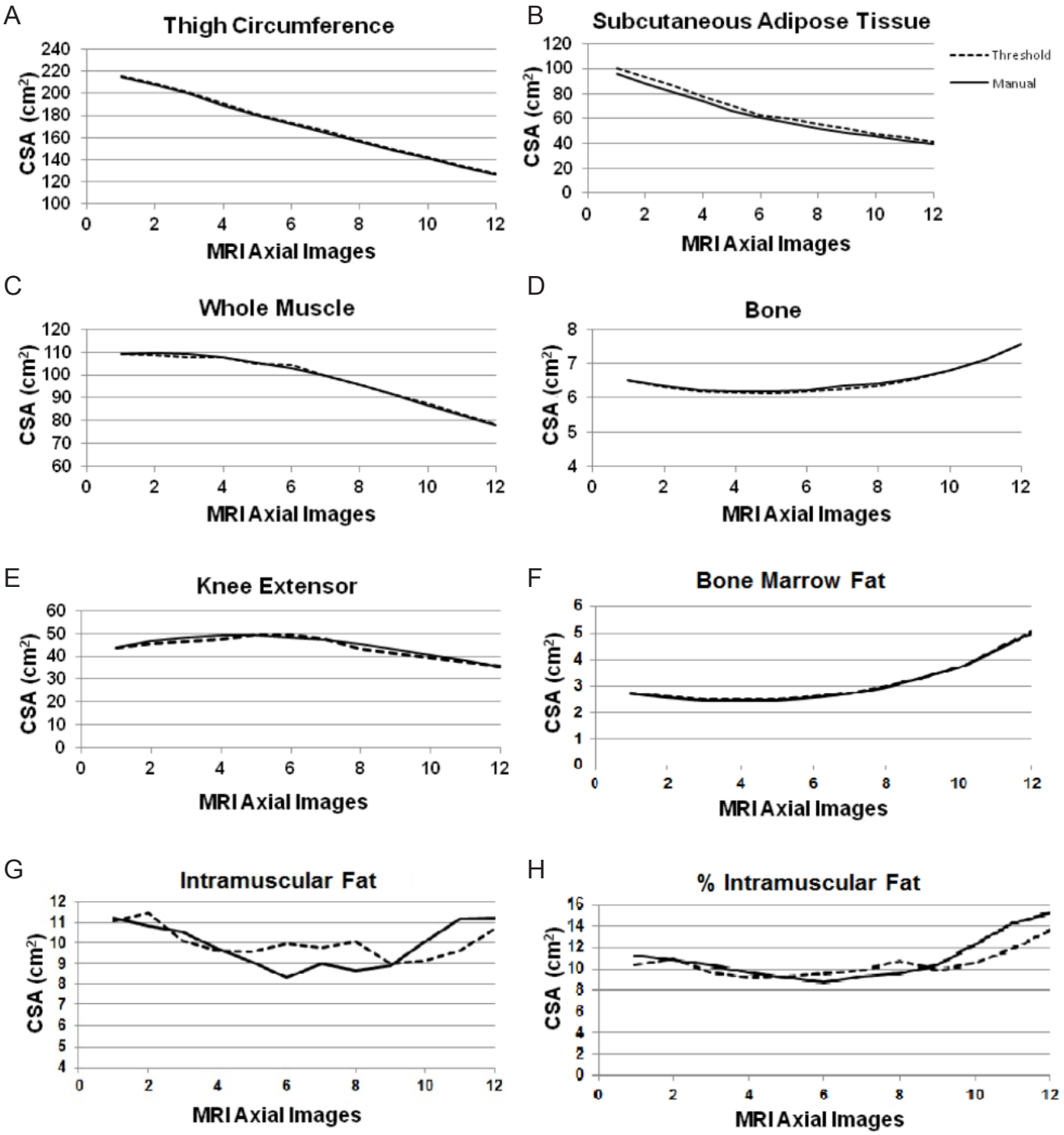

Figure 3 The average CSA of multi-axial slices from the hip (image # 1) to the knee (image # 12) joints comparing both manual and threshold techniques for (A) TC, (B) SAT, (C) WM, (D) femoral bone, (E) KE, (F) BMF, (G) IMF and (H) %IMF ROIs.
Slice number from the hip to knee joints is plotted along the x-axis. Each data point corresponds to the average CSA (cm^2) of 18 men. CSA: Cross-sectional area; TC: Thigh circumference; SAT: subcutaneous adipose tissue; WM: whole muscle; KE: knee extensor; BMF: bone marrow fat; IMF: intramuscular fat; ROI: region of interest; MRI: magnetic resonance imaging.

compartments (see below).

Previous studies have used MRI as the "gold-standard" technique for measuring changes in muscle composition after SCI and in response to exercise interventions (Mitsiopoulos et al., 1985; Elder et al., 2004; Gorgey and Dudley, 2007; Gorgey et al., 2012). A major disadvantage of the manual tracing technique is the extensive time required to analyze multi-axial slices especially in large clinical trials (Modlesky et al., 2004). The process of manually tracing is also expensive and may require more than one person to work on the same project to complete the task in a timely manner. This is likely to influence the precision of the technique and introduce a source of unaccountable error.

As computer programming and software systems develop, MRI tissue quantification continues towards more automated approaches in an effort to reduce analysis time (Urricelqui

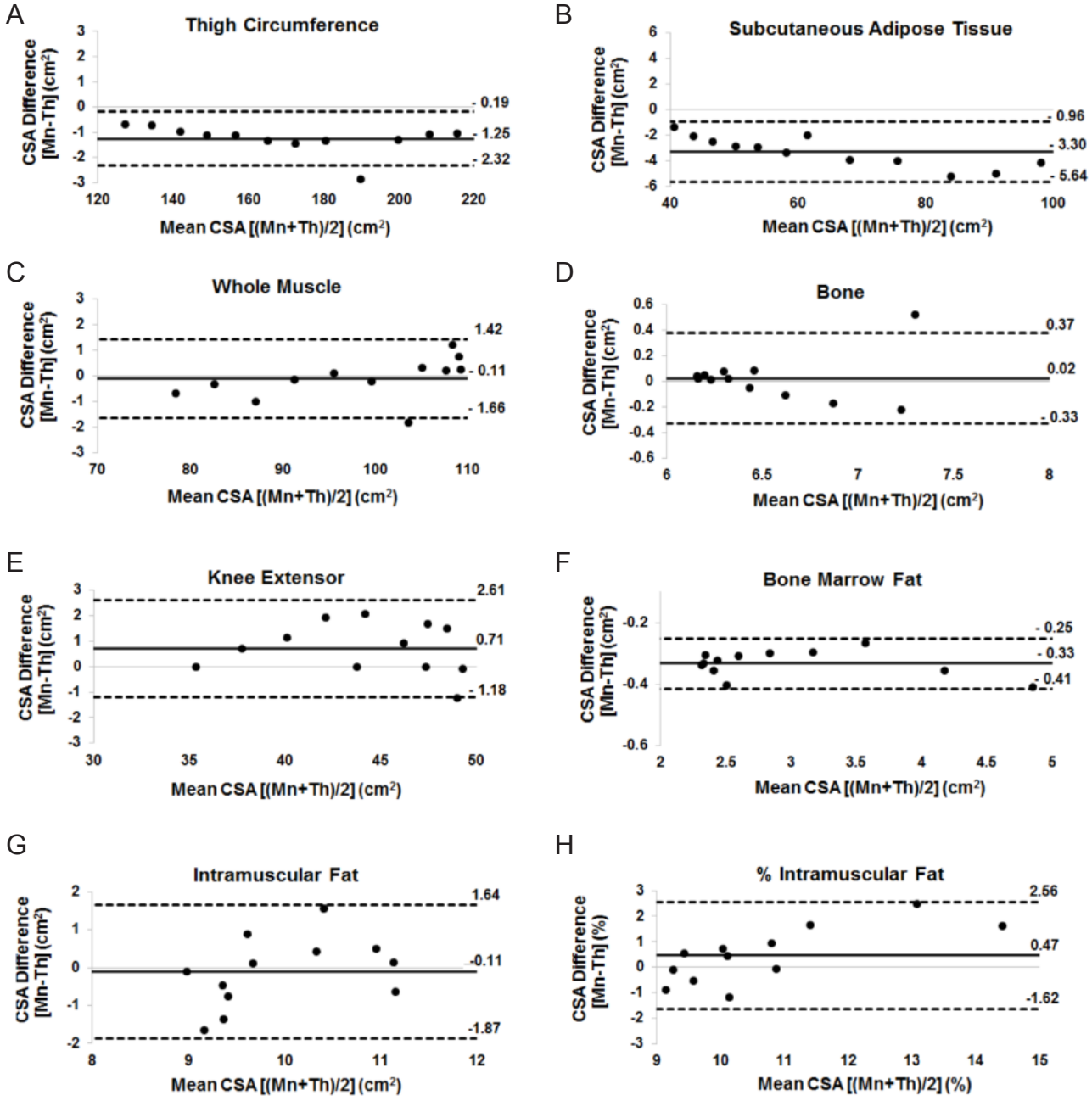

Figure 4 Bland-Altman plots showing levels of agreement between manual (Mn) and threshold (Th) techniques for (A) TC, (B) SAT, (C) WM, (D) femoral bone, (E) KE, (F) BMF, (G) IMF and (H) %IMF ROIs.
Each data point corresponds to the average CSA (cm^2) of 18 men. CSA: Cross-sectional area; TC: Thigh circumference; SAT: subcutaneous adipose tissue; WM: whole muscle; KE: knee extensor; BMF: bone marrow fat; IMF: intramuscular fat; ROI: region of interest.

et al., 2009; Purushwalkam et al., 2013; Orgiu et al., 2016). For example, quantifying thigh compartments using manual segmentation for the seven ROIs requires ~25 minutes per image and ~5 hours to complete analysis of one subject depending on the number of images per sequence (leg length) and image resolution. Using the semi-automated threshold technique, a total of 216 images were analyzed in one hour per subject and was capable of cutting the analysis time by ~80% while maintaining a robust accuracy.

Despite other research studies that have documented that the threshold technique may be highly sensitive and reliable in abled-bodied subjects (Urricelqui et al., 2009; Purushwalkam et al., 2013; Orgiu et al., 2016), SCI patients represent an ideally challenging population because they are characterized by extreme muscle atrophy and infiltration of IMF (**Figure 1B**) (Elder et al., 2004; Gorgey et al., 2013a, 2015). This results in significant architectural changes, which may require additional validation to any previously developed threshold program. Therefore, extrapolating results from able-bodied studies to persons with SCI is not a

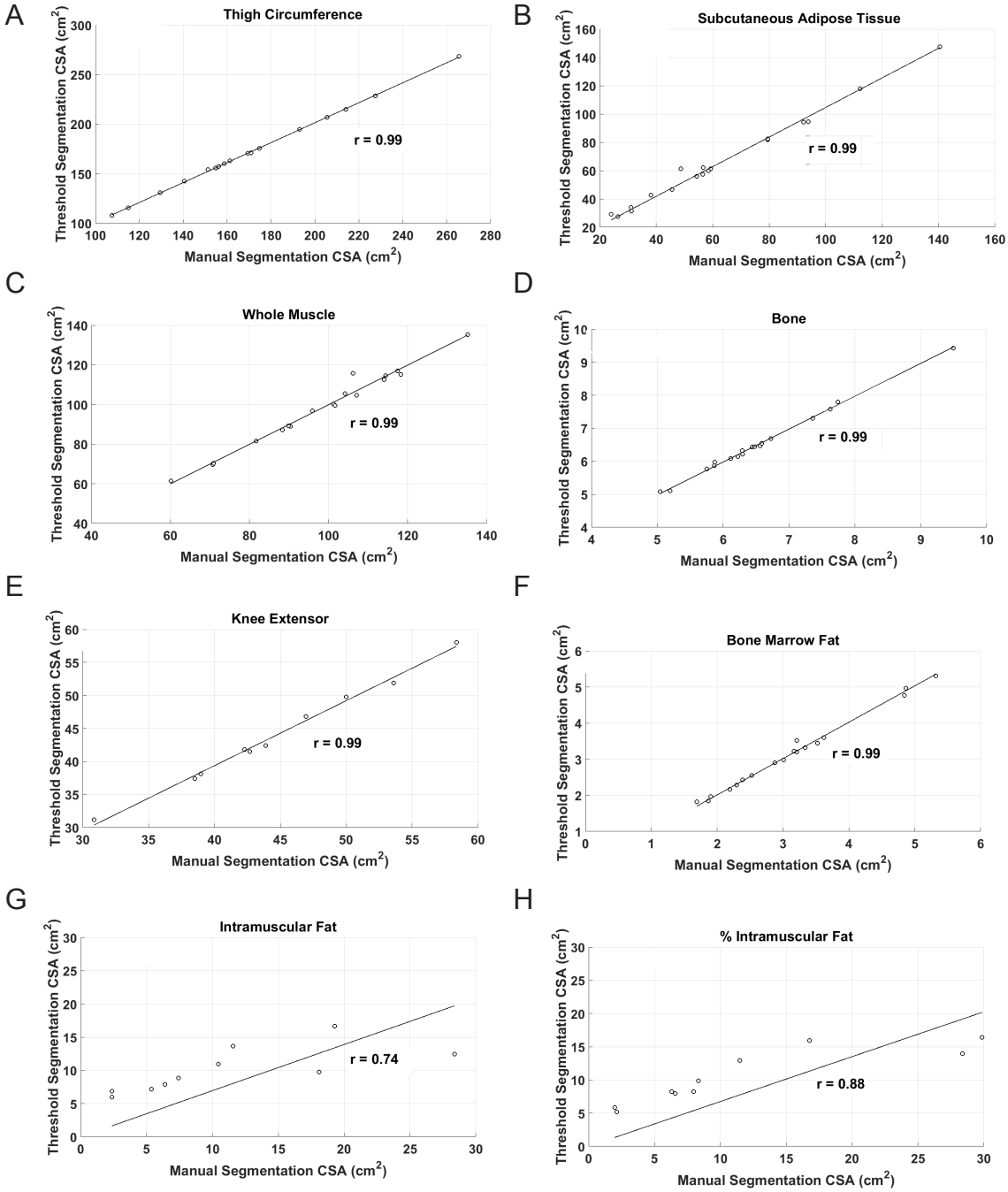

Figure 5 Linear regression showing relationships between manual and threshold CSA values for each individual image for (A) TC, (B) SAT, (C) WM, (D) femoral bone, (E) KE, (F) BMF, (G) IMF and (H) %IMF ROIs.

CSA: cross-sectional area; TC: thigh circumference; SAT: subcutaneous adipose tissue; WM: whole muscle; KE: knee extensor; BMF: bone marrow fat; IMF: intramuscular fat.

feasible or acceptable approach. We chose to run the average of MRI slices rather than the average muscle CSA of each participant. This was accomplished to highlight the error in spatial distribution of the different tissues along the entire thigh length from the hip to the knee joints. For example, in **Figure 4**, the Bland-Altman shows that for each of the WM, SAT, bone ROIs, the error slightly increased towards the knee joint, this means that the sensitivity of the threshold technique may be influenced by the anatomical distribution of muscle and SAT regions.

This is likely also to explain the wide level of agreement in SAT and %IMF. For WM segmentation, the method was based on the assumption that the fascial line is adherent to the muscle wall of the thigh, which is true in most abled-bodied individuals; however, after SCI, this fascial line may be pushed outward from the muscle wall because of the infiltrated subfascial fat subfascial fat and IMF. This may explain the highest percentage error in SAT (5.22%). Reliance on the geometrical structure of thigh compartments to determine the orientation of the fascial line was necessary

because the lack of signal intensity discrepancy between the fascia and muscle pixels while using the threshold technique. Similar studies have presented more automated methods for thigh tissue quantification, yet such approaches require higher programming skills, more complex software and sophisticated image processing tools (Urricelqui et al., 2009; Purushwalkam et al., 2013; Orgiu et al., 2016). that require technical expertise, not often available in clinical research laboratories investigating body composition. However, a main strength of the current segmentation technique is a free tool and easily accessible in open source library tool, without the need to extensive technical skills or training efforts. Future studies should develop automated techniques that quantify both IMF and subfascial fat to provide more accurate delineation of SAT based on the facial line.

The current study has addressed several of the inherited weakness in previous studies. A previous study had mixed populations of able-bodied, elderly and obese individuals and one study showed lower accuracy in the obese population (77.5%) when compared to manual tracing segmentation (Orgiu et al., 2016). Another study used Image J software and threshold segmentation to quantify adipose tissue of the calf and thigh. However, the results obtained from threshold segmentation were not compared to manual tracing to verify the accuracy of the approach and the study enrolled only 6 participants (Al-Attar et al., 2006). These studies have refrained from analyzing individual muscle groups of the thigh due to difficulty indiscriminate anatomical border of individual muscle group. The current technique may provide a great advantage to study the changes in individual muscle size in response to different training, pharmaceutical and dietary interventions, which is of relatively high clinical relevance to the current population (Dolbow et al., 2017; Gorgey et al., 2017b).

Limitations

The sample size was relatively small (n = 18), however, the proposed method can be reproduced in greater numbers in individuals with abled bodied or chronic SCI. Future trials should investigate imaging of both men and women with SCI; however, a predominantly male sample should not directly limit the effectiveness of the current method (Gorgey et al., 2017b). We have primarily included men because the parent study was designed to investigate the effects of resistance training and testosterone replacement therapy in men with SCI. The proposed method will analyze additional individual muscle groups of the thigh including the hip adductors and knee flexors. Muscles of the lower leg will also be segmented using the threshold technique to determine the CSAs of the gastrocnemius and soleus muscles, which are associated with deficiencies in calf muscle pump activity, lower body circulation and chronic heart failure in persons with SCI (Lester et al., 2017). Moreover, threshold derived segmentation will be applied to visceral compartments to quantify visceral adipose tissue and trunk muscle CSAs. Evidence suggests that these two ROI are associated with increasing risks of metabolic dysfunction, insulin resistance and type II diabetes in both SCI and abled-bodied populations (Duckworth et al., 1980; Gater, 2007; Gorgey et al., 2014, 2015). We have relied primarily on T1-weighted MRI, because this was the fundamental MRI protocol that was used previously in delineating the anatomical boundaries. However, several imaging sequences are now available similar to fat fraction technique that should be tested in future studies.

Conclusion

Threshold technique provided a robust quantification and speedy assessment of thigh muscle and fat CSAs compared to the standard manual tracing technique in persons with SCI. More automated segmentation of thigh muscle and fat compartments will allow researchers to efficiently assess muscle size and IMF infiltration in a fraction of the time previously required for manual tracing technique. This may allow for faster diagnostics and the development of a more individualized rehabilitation strategy designed around improving body composition and preventing the occurrence of metabolic abnormalities after SCI.

Acknowledgments: *We would like to thank the participants who devoted the time and effort to participate in the current study. We would like to thank Hunter Holmes McGuire Research Institute and Spinal Cord Injury Services and Disorders for providing the environment to conduct clinical human research trials.*

Conflicts of interest: *The authors declare that they have no conflicts of interest.*

Financial support: *This study was supported by the Department of Veteran Affairs, Veteran Health Administration, Rehabilitation Research and Development Service (B7867-W) and DoD-CDRMP (W81XWH-14-SCIRP-CTA) (to ASG). The funding body played no role in the study conception design, in the collection, analysis and interpretation of data, in the preparation and writing of paper, and in the decision to submit the paper for publication.*

Institutional review board statement: *All study procedures were approved by the Institutional Review Board (McGuire IRB#1) and conducted according to the Declaration of Helsinki.*

Declaration of patient consent: *The authors certify that they have obtained all appropriate patient consent forms. In the form the patients have given their consent for their images and other clinical information to be reported in the journal. The patients understand that their names and initials will not be published and due efforts will be made to conceal their identity.*

Reporting statement: *This study follows the Strengthening the Reporting of Observational Studies in Epidemiology (STROBE) statement.*

Biostatistics statement: *The statistical methods of this study were reviewed by the biostatistician of Hunter Holmes McGuire VA Medical Center in Richmond, VA, USA.*

Copyright license agreement: *The Copyright License Agreement has been signed by all authors before publication.*

Data sharing statement: *The individual participant data is available. Individual participant data that underlie the results reported in this article, after deidentification will be shared. Study Protocol, Informed Consent Form, and Clinical Study Report will be available. Data will be available beginning 9 months and ending 36 months following article publication. Investigations whose proposed use of the data has been approved by an independent review committee ("learned intermediary") identified for this purpose. The shared data will be used for individual participant data meta-analysis. Proposals may be submitted up to 36 months following article publication. After 36 months the data will be available in our University's data warehourse but without investigator support other than deposited metadata. Information regarding submitting proposals and accessing data may be found at (Link to be provided).*

Plagiarism check: *Checked twice by iThenticate.*

Peer review: *Externally peer reviewed.*

Open peer reviewers: *Mitsuhiro Enomoto, Tokyo Medical and Dental University, Japan; Tania Cristina Leite de Sampaio e Spohr, Instituto Estadual do Cérebro Paulo Niemeyer, Brazil.*
Additional file: *Open peer review reports 1 and 2.*

References

Al-Attar SA, Pollex RL, Robinson JF, Miskie BA, Walcarius R, Rutt BK, Hegele RA (2006) Semi-automated segmentation and quantification of adipose tissue in calf and thigh by MRI: a preliminary study in patients with monogenic metabolic syndrome. BMC Medical Imaging 6:11.

Barber CB, Dobkin DP, Huhdanpaa HT (1996) The Quickhull Algorithm for Convex Hulls. ACM Trans Math Softw 22:469-483.

Buchholz AC, McGillivray CF, Pencharz PB (2003) Physical activity levels are low in free-living adults with chronic paraplegia. Obes Res 11:563-570.

Buchholz AC, Pencharz PB (2004) Energy expenditure in chronic spinal cord injury. Curr Opin Clin Nutr Metab Care 7:635-639.

Castro MJ, Apple DF Jr, Hillegass EA, Dudley GA (1999) Influence of complete spinal cord injury on skeletal muscle cross-sectional area within the first 6 months of injury. Eur J Appl Physiol Occup Physiol 80:373-378.

Cormen TH, Leiserson CE, Rivest RL, Stein C (2001) Introduction to Algorithms. 2nd ed. Cambridge, MA: MIT Press.

Dolbow DR, Gorgey AS, Khalil RK, Gater DR (2017) Effects of a fifty-six month electrical stimulation cycling program after tetraplegia: case report. J Spinal Cord Med 40:485-488.

Duckworth WC, Solomon SS, Jallepalli P, Heckemeyer C, Finnern J, Powers A (1980) Glucose intolerance due to insulin resistance in patients with spinal cord injuries. Diabetes 29:906-910.

Dudley-Javoroski S, Shields RK (2012) Regional cortical and trabecular bone loss after spinal cord injury. J Rehabil Res Dev 49:1365-1376.

Elder CP, Apple DF, Bickel CS, Meyer RA, Dudley GA (2004) Intramuscular fat and glucose tolerance after spinal cord injury--a cross-sectional study. Spinal Cord 42:711-716.

Eser P, Frotzler A, Zehnder Y, Wick L, Knecht H, Denoth J, Schiessl H (2004) Relationship between the duration of paralysis and bone structure: a pQCT study of spinal cord injured individuals. Bone 34:869-880.

Fattal C, Mariano-Goulart D, Thomas E, Rouays-Mabit H, Verollet C, Maimoun L (2011) Osteoporosis in persons with spinal cord injury: the need for a targeted therapeutic education. Arch Phys Med Rehabil 92:59-67.

Fortin M, Omidyeganeh M, Battié MC, Ahmad O, Rivaz H (2017) Evaluation of an automated thresholding algorithm for the quantification of paraspinal muscle composition from MRI images. Biomed Eng Online 16:61.

Gater DR (2007) Jr Obesity after spinal cord injury. Phys Med Rehabil Clin N Am 8:333-351.

Gorgey AS, Dudley GA (2007) Skeletal muscle atrophy and increased intramuscular fat after incomplete spinal cord injury. Spinal Cord 45:304-309.

Gorgey AS, Mather KJ, Gater DR (2011a) Central adiposity associations to carbohydrate and lipid metabolism in individuals with complete motor spinal cord injury. Metabolism 60:843-851.

Gorgey AS, Mather KJ, Poarch HJ, Gater DR (2011b) Influence of motor complete spinal cord injury on visceral and subcutaneous adipose tissue measured by multi-axial magnetic resonance imaging. J Spinal Cord Med 34:99-109.

Gorgey AS, Mather KJ, Cupp HR, Gater DR (2012) Effects of resistance training on adiposity and metabolism after spinal cord injury. Med Sci Sports Exerc 44:165-174.

Gorgey AS, Dolbow DR, Cifu DX, Gater DR (2013a) Neuromuscular electrical stimulation attenuates thigh skeletal muscles atrophy but not trunk muscles after spinal cord injury. J Electromyogr Kinesiol 23:977-984.

Gorgey AS, Poarch HJ, Adler RA, Khalil RE, Gater DR (2013b) Femoral bone marrow adiposity and cortical bone cross-sectional areas in men with motor complete spinal cord injury. PM R 5:939-948.

Gorgey AS, Dolbow DR, Dolbow JD, Khalil RK, Castillo C, Gater DR (2014) Effects of spinal cord injury on body composition and metabolic profile - part I. J Spinal Cord Med 37:693-702.

Gorgey AS, Wells KM, Austin TL (2015) Adiposity and spinal cord injury. World J Orthop 6:567-576.

Gorgey AS, Moore PD, Wade RC, Gill RS, Lavis T, Adler RA (2017a) Disruption in bone marrow fat may attenuate testosterone action on muscle size after spinal cord injury. A case report. Eur J Phys Rehabil Med 53:625-629.

Gorgey AS. Khalil RE, Gill R, O'Brien LC, Lavis T, Castillo T, Cifu DX, Savas J, Khan R, Cardozo C, Lesnefsky EJ, Gater DR, Adler RA (2017b) Effects of Testosterone and Evoked Resistance Exercise after Spinal Cord Injury (TEREX-SCI): study protocol for a randomised controlled trial. BMJ Open 7:e014125.

Lester RM, Johnson K, Khalil RE, Khan R, Gorgey AS (2017) MRI analysis and clinical significance of lower extremity muscle cross-sectional area after spinal cord injury. Neural Regen Res 12:714-722.

Mitsiopoulos N, Baumgartner RN, Heymsfield SB, Lyons W, Gallagher D, Ross R (1985) Cadaver validation of skeletal muscle measurement by magnetic resonance imaging and computerized tomography. J Appl Physiol 85:115-122.

Modlesky CM, Bickel CS, Slade JM, Meyer RA, Cureton KJ, Dudley GA (2004) Assessment of skeletal muscle mass in men with spinal cord injury using dual-energy X-ray absorptiometry and magnetic resonance imaging. J Appl Physiol (1985) 96:561-565.

Monroe MB, Tataranni PA, Pratley R, Manore MM, Skinner JS, Ravussin E (1998) Lower daily energy expenditure as measured by respiratory chamber in subjects with spinal cord injury compared with control subjects. Am J Clin Nutr 68:1223-1227.

Moore PD, Gorgey AS, Wade RC, Khalil RE, Lavis TD, Khan R, Adler RA (2016) Neuromuscular electrical stimulation and testosterone did not influence heterotopic ossification size after spinal cord injury: A case series. World J Clin Cases 4:172-176.

Olle MM, Pivarnik JM, Klish WJ, Morrow JR (1993) Body composition of sedentary and physically active spinal cord injured individuals estimated from total body electoral conductivity. Arch Phys Med Rehabil 74:706-710.

Orgiu S, Lafortuna CL, Rastelli F, Cadioli M, Falini A and Rizzo G (2016) Automatic muscle and fat segmentation in the thigh from T1-Weighted MRI. J Magn Reson Imaging 43:601-610.

Phillips WT, Kiratli BJ, Sarkarati M, Weraarchakul G (1998) Effects of spinal cord injury on the heart and cardiovascular fitness. Curr Prob Cardiol 23:641-716.

Prescott JW, Priddy M, Best TM, Pennell M, Swanson MS, Haq F, Jackson RD, Gurcan MN (2009) An automated method to detect interstitial adipose tissue in thigh muscles for patients with osteoarthritis. Conf Proc IEEE Eng Med Biol Soc 1:6360-6363.

Purushwalkam S, Li B, Meng Q, McPhee J (2013) Automatic Segmentation of adipose tissue from thigh magnetic resonance images. ICIAR 451-458.

Qin W, Bauman WA, Cardozo CP (2010) Evolving concepts in neurogenic osteoporosis. Curr Osteoporos Rep 8:212-218.

Schick F (2016) Tissue segmentation: a crucial tool for quantitative MRI and visualization of anatomical structures. MAGMA 29:89-93.

Sedlock DA, Laventure SJ (1990) Body composition and resting energy expenditure and basal metabolic rates of patients with spinal cord injury. Paraplegia 28:448-454.

Singh PK, Sharma G, Pandey PK (2017) Watershed Algorithm and Adaptive Threshold Canny Edge Detection Based Automatic Segmentation of Tibio Femoral Cartilage from MRI Images. Biosci Biotech Res Asia 14:843-852.

Urricelqui L, Malanda A, Villanueva A (2009) Automatic segmentation of thigh magnetic resonance images. WASET Congress 58:979.

Wilmet E, Ismail AA, Heilporn A, Welraeds D, Bergmann P (1996) Longitudinal study of bone mineral content and soft tissue composition after spinal cord section. Paraplegia 33:674-677.